ARTICLE

doi:10.1038/nature14967

Mapping tree density at a global scale

T. W. Crowther[1], H. B. Glick[1], K. R. Covey[1], C. Bettigole[1], D. S. Maynard[1], S. M. Thomas[2], J. R. Smith[1], G. Hintler[1], M. C. Duguid[1], G. Amatulli[3], M.-N. Tuanmu[3], W. Jetz[1,3,4], C. Salas[5], C. Stam[6], D. Piotto[7], R. Tavani[8], S. Green[9,10], G. Bruce[9], S. J. Williams[11], S. K. Wiser[12], M. O. Huber[13], G. M. Hengeveld[14], G.-J. Nabuurs[14], E. Tikhonova[15], P. Borchardt[16], C.-F. Li[17], L. W. Powrie[18], M. Fischer[19,20], A. Hemp[21], J. Homeier[22], P. Cho[23], A. C. Vibrans[24], P. M. Umunay[1], S. L. Piao[25], C. W. Rowe[1], M. S. Ashton[1], P. R. Crane[1] & M. A. Bradford[1]

The global extent and distribution of forest trees is central to our understanding of the terrestrial biosphere. We provide the first spatially continuous map of forest tree density at a global scale. This map reveals that the global number of trees is approximately 3.04 trillion, an order of magnitude higher than the previous estimate. Of these trees, approximately 1.39 trillion exist in tropical and subtropical forests, with 0.74 trillion in boreal regions and 0.61 trillion in temperate regions. Biome-level trends in tree density demonstrate the importance of climate and topography in controlling local tree densities at finer scales, as well as the overwhelming effect of humans across most of the world. Based on our projected tree densities, we estimate that over 15 billion trees are cut down each year, and the global number of trees has fallen by approximately 46% since the start of human civilization.

Forest ecosystems harbour a large proportion of global biodiversity, contribute extensively to biogeochemical cycles, and provide countless ecosystem services, including water quality control, timber stocks and carbon sequestration[1–4]. Our current understanding of the global forest extent has been generated using remote sensing approaches that provide spatially explicit values relating to forest area and canopy cover[3,5,6]. Used in a wide variety of global models, these maps have enhanced our understanding of the Earth system[3,5,6], but they do not currently address population numbers, densities or timber stocks. These variables are valuable for the modelling of broad-scale biological and biogeochemical processes[7–9] because tree density is a prominent component of ecosystem structure, governing elemental processing and retention rates[7,9,10], as well as competitive dynamics and habitat suitability for many plant and animal species[11–13].

The number of trees in a given area can also be a meaningful metric to guide forest management practices and inform decision-making in public and non-governmental sectors[14,15]. For example, international afforestation efforts such as the 'Billion Trees Campaign', and city-wide projects including the numerous 'Million Tree' initiatives around the world have motivated civil society and political leaders to promote environmental stewardship and sustainable land management by planting large numbers of trees[14,16,17]. Establishing targets and evaluating the proportional contribution of such projects requires a sound baseline understanding of current and potential tree population numbers at regional and global scales[16,17].

The current estimate of global tree number is approximately 400.25 billion[18]. Generated using satellite imagery and scaled based on global forest area, this estimate engaged policy makers and environmental practitioners worldwide by suggesting that the ratio of trees-to-people is 61:1. This has, however, been thrown into doubt by a recent broad-scale inventory that used 1,170 ground-truthed measurements of tree density to estimate that there are 390 billion trees in the Amazon basin alone[19].

Mapping tree density

Here, we use 429,775 ground-sourced measurements of tree density from every continent on Earth except Antarctica to generate a global map of forest trees. Forested areas are found in most of Earth's biomes, even those as counterintuitive as desert, tundra, and grassland (Fig. 1a, b). We generated predictive regression models for the forested areas in each of the 14 biomes as defined by The Nature Conservancy (http://www.nature.org). These models link tree density to spatially explicit remote sensing and geographic information systems (GIS) layers of climate, topography, vegetation characteristics and anthropogenic land use (see Extended Data Table 1). Following almost all of the collected data sources, we define a tree as a plant with woody stems larger than 10 cm diameter at breast height (DBH)[19].

Incorporating plot-level measurements from more than 50 countries, the measured tree density values were inherently variable within and among biomes (Figs 1 and 2). However, the large number of tree density measurements ensured that the confidence in our mean (and total) estimates is high (Fig. 3). Furthermore, the scale of these data

[1]Yale School of Forestry and Environmental Studies, Yale University, New Haven, Connecticut 06511, USA. [2]Department of Environmental Sciences, University of Helsinki, Helsinki 00014, Finland. [3]Department of Ecology and Evolutionary Biology, Yale University, New Haven, Connecticut 06511, USA. [4]Department of Life Sciences, Silwood Park, Imperial College, London SL5 7PY, UK. [5]Departamento de Ciencias Forestales, Universidad de La Frontera, Temuco 4811230, Chile. [6]RedCastle Resources, Salt Lake City, Utah 84103, USA. [7]Universidade Federal do Sul da Bahia, Ferradas, Itabuna 45613-204, Brazil. [8]Forestry Department, Food and Agriculture Organization of the United Nations, Rome 00153, Italy. [9]Operation Wallacea, Spilbsy, Lincolnshire PE23 4EX, UK. [10]Durrell Institute of Conservation and Ecology (DICE), School of Anthropology and Conservation (SAC), University of Kent, Canterbury ME4 4AG, UK. [11]Molecular Imaging Research Center MIRCen/CEA, CNRS URA 2210, 91401 Orsay Cedex, France. [12]Landcare Research, Lincoln 7640, New Zealand. [13]WSL, Swiss Federal Institute for Forest, Snow and Landscape Research, 8903 Birmensdorf, Switzerland. [14]Environmental Science Group, Wageningen University & Research Centre, 6708 PB, The Netherlands. [15]Center for Forest Ecology and Productivity RAS, Moscow 117997, Russia. [16]CEN Center for Earth System Research and Sustainability, Institute of Geography, University of Hamburg, Hamburg 20146, Germany. [17]Department of Botany and Zoology, Masaryk University, Brno 61137, Czech Republic. [18]South African National Biodiversity Institute, Kirstenbosch Research Centre, Claremont 7735, South Africa. [19]Institute of Plant Sciences, Botanical Garden, and Oeschger Centre for Climate Change Research, University of Bern, 3013 Bern, Switzerland. [20]Senckenberg Gesellschaft für Naturforschung, Biodiversity and Climate Research Centre (BIK-F), 60325 Frankfurt, Germany. [21]Department of Plant Systematics, University of Bayreuth, 95447 Bayreuth, Germany. [22]Albrecht von Haller Institute of Plant Sciences, Georg August University of Göttingen, 37073 Göttingen, Germany. [23]Tropical Ecology Research Group, Lancaster Environment Centre, Lancaster University, Lancaster LA1 4YQ, UK. [24]Universidade Regional de Blumenau, Departamento de Engenharia Florestal, Blumenau/Santa Catarina 89030-000, Brazil. [25]Sino-French Institute for Earth System Science, College of Urban and Environmental Sciences, Peking University, Beijing 100871, China.

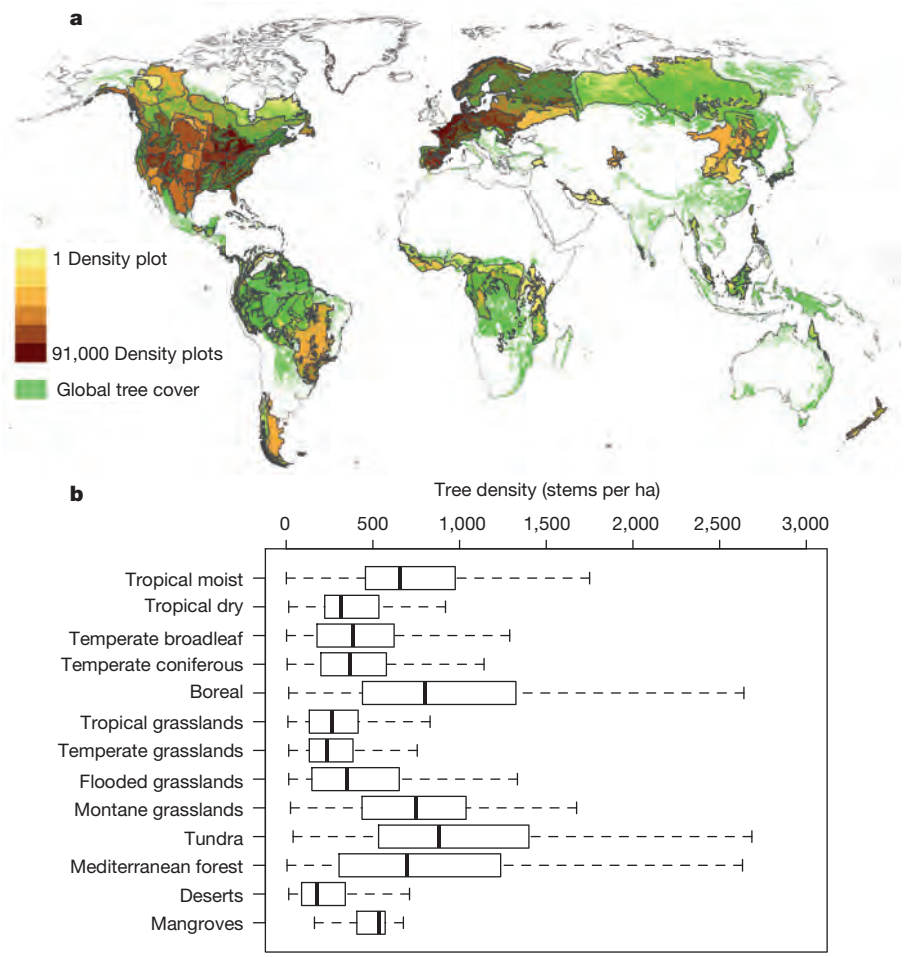

Figure 1 | Map of data points and raw biome-level forest density data. **a**, Image highlighting the ecoregions (shapefiles provided by The Nature Conservancy (http://www.nature.org)) from which the 429,775 ground-sourced measurements of tree density were collected. Shading indicates the total number of plot measurements collected in each ecoregion. A global forest map was overlaid in green to highlight that collected data span the majority of forest ecosystems on a global scale. **b**, The median and interquartile range of tree density values collected in the forested areas of each biome.

ensures that our modelled estimates are unlikely to be influenced significantly by recent forest loss, reforestation or natural forest regeneration, which are responsible for a net global change of <1% of the global forest area each year[3]. Biome-level validation estimates indicate that our models have high precision when predicting the mean tree densities of omitted validation plots (Fig. 3a). Although the accuracy

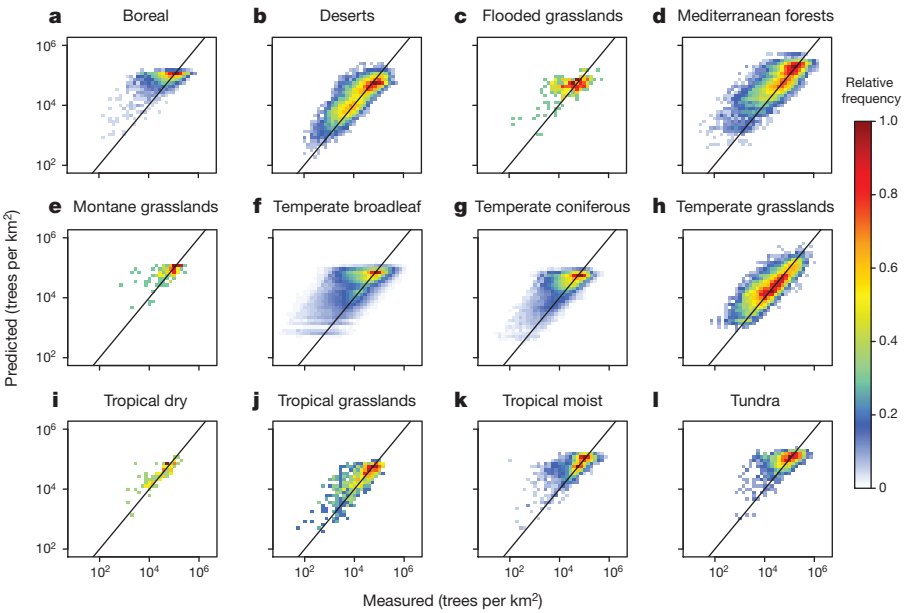

Figure 2 | Heat plots showing the relationships between predicted and measured tree density data. **a**–**l**, Predictions were generated using generalized linear models (n = 429,775). Diagonal lines indicate 1:1 lines (perfect correspondence) between predicted and observed points, scaled to the kilometre level. Colours indicate the proportion of data points from that biome that fall within each pixel. Biomes with a greater number of plot measurements have greater variability but higher confidence in the mean estimates, highlighting the trade-off between broad-scale precision and fine-scale accuracy. Axes are log-transformed to account for exceptionally high variability in tree density.

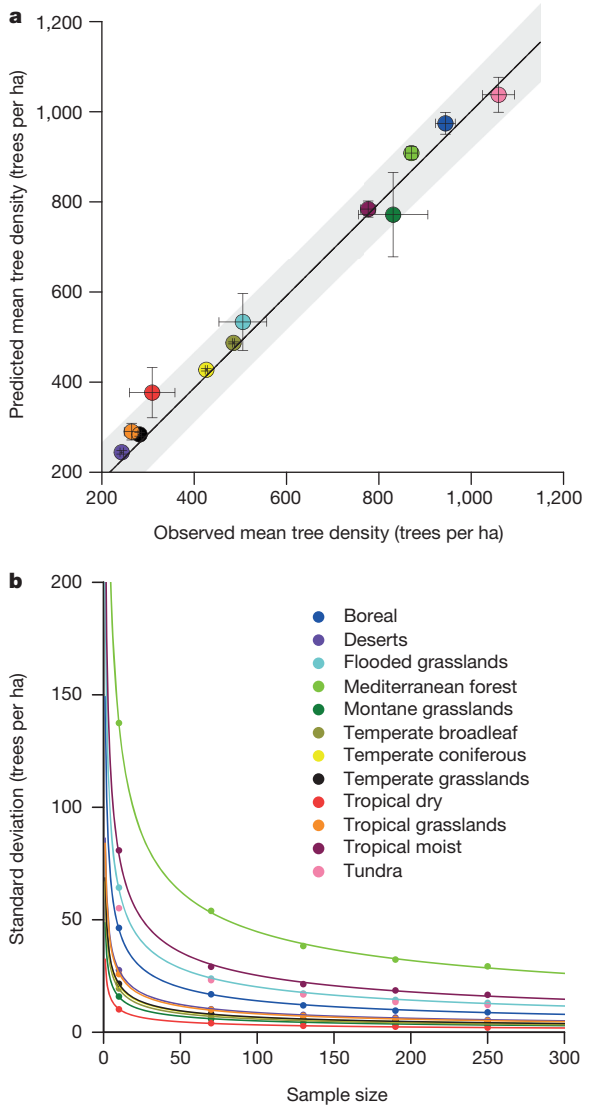

Figure 3 | Validation plots for biome-level predictions. **a**, Biome-level regression models predict the mean values of the omitted validation plot measurements in 12 biomes. Overall, the models underestimated mean tree density by ~3% (slope = 0.97) but this difference was not statistically significant ($P = 0.51$). Bars show ± one standard deviation for the predicted mean and the grey area represents the 95% confidence interval for the mean. The values plotted here represent mean densities for the plot measurements (that is, for forested ecosystems), rather than those predicted for each entire biome. **b**, The standard deviation of the predicted mean values as a function of sample size. As sample size increases, the variability of the predicted mean tree density reaches a threshold, beyond which an increase in sample size results in a minimal increase in precision. Standard deviations were calculated using a bootstrapping approach (see Methods), and smooth curves were modelled using standard linear regression with a log–log transformation.

of our models is limited at the level of an individual hectare, the precision of the mean density estimates is high (±40 trees ha^{-1}) beyond a threshold of ~200 plots (Fig. 3b).

Global-level and biome-level patterns

Together, the biome-level models provide the first spatially continuous map of global tree densities at a 1-km^2 (30 arc-seconds) resolution (Fig. 4a). Based on this map, we estimate that the global number of trees is approximately 3.04 trillion (±0.096 trillion, 95% confidence intervals (CI)). An order of magnitude higher than the previous global estimate[18], the scale of our projection is consistent with recent large-scale inventories in Europe, North America and the Amazon basin[19] (Fig. 4d). With a human population of 7.2 billion, our estimate of global tree density revises the ratio of trees per person from 61:1 to 422:1.

At the biome-level, the highest tree densities exist in forested regions of the Boreal and Tundra zones (Fig. 1b). In these northern latitudes, limited temperature and moisture lead to the establishment of stress-tolerant coniferous tree species that can reach the highest densities on Earth (Fig. 1). However, the tropical regions contain a greater proportion of the world's forested land. A total of 42.8% of the planet's trees exist in tropical and subtropical regions, with another 24.2% and 21.8% in boreal and temperate biomes, respectively (Fig. 4a).

Within-biome trends

Our models also provide mechanistic insights into potential controls on tree density within biomes (Fig. 5). For example, various climatic parameters correlate with mean forest density within all ecosystem types. Tree density generally increases with temperature (mean annual temperature and temperature seasonality) and moisture availability (precipitation regimes, evapotranspiration or aridity). These patterns are consistent with previous broad-scale tree inventory studies and support the idea that, within ecosystem types, moist, warm conditions are generally optimal for tree growth[11,12].

Given the generally positive effects of moisture availability and warmth on tree density within biomes, the negative relationships observed in some regions may seem surprising (Fig. 5). This highlights the complex suite of population- and community-level selection pressures that can obscure the expected effects of climate across landscapes. For example, in colder (boreal or tundra) biomes, increasing moisture levels can cause hydric and permafrost conditions in lower lying topographies, which then limit nutrient availability for tree development[20]. In addition, current and historical anthropogenic land use decisions have the potential to drive these relationships in several regions. The negative relationships between tree density and moisture availability in flooded grasslands and tropical dry forests are, for example, likely to be driven by preferential use of moist, productive land for agriculture[21]. As a result, forest ecosystems are often relegated to drier regions, reversing the expected within-biome relationships between moisture availability and tree density. Such effects will vary among countries, depending on human population densities, alternative resource availability and socio-economic status[22,23].

Along with these indirect effects of human activity, the direct effect of human development (percentage developed and managed land)[6] on tree density represented the only common mechanism across all biomes (Fig. 5). The negative relationships between tree density and anthropogenic land use exemplify how humans contend directly with natural forest ecosystems for space. Whereas the negative effect of human activity on tree numbers is highly apparent at local scales, the present study provides a new measure of the scale of anthropogenic effects, relative to other environmental variables. Current rates of global forest cover loss are approximately 192,000 km^2 each year[3]. By combining our tree density information with the most recent spatially explicit map of forest cover loss over the past 12 years[3], we estimate that deforestation, forest management, disturbances and land use change are currently responsible for a gross loss of approximately 15.3 billion trees on an annual basis. Although these rates of forest loss are currently highest in tropical regions[3], the scale and consistency of this negative human effect across all forested biomes highlights how historical land use decisions have shaped natural ecosystems on a global scale. Using the projected maps of current and historic forest cover provided by the United Nations Environment Programme (http://geodata.grid.unep.ch), our map reveals that the global number of trees has fallen

a

Terrestrial biome (number of ground-sourced density estimates)	Total trees (billions) ± 95% CI
Boreal forests (*n* = 8,688)	749.3 (± 50.1)
Deserts (*n* = 14,637)	53.0 (± 2.9)
Flooded grasslands (*n* = 271)	64.6 (± 14.2)
Mangroves (*n* = 21)	8.2 (± 0.3)
Mediterranean forests (*n* = 16,727)	53.4 (± 1.2)
Montane grasslands (*n* = 138)	60.3 (± 24.0)
Temperate broadleaf (*n* = 278,395)	362.6 (± 2.9)
Temperate conifer (*n* = 85,144)	150.6 (± 1.3)
Temperate grasslands (*n* = 17,051)	148.3 (± 4.9)
Tropical coniferous (*n* = 0)	22.2 (± 0.4)
Tropical dry (*n* = 115)	156.4 (± 63.4)
Tropical grasslands (*n* = 999)	318.0 (± 35.5)
Tropical moist (*n* = 5,321)	799.4 (± 24.0)
Tundra (*n* = 2,268)	94.9 (± 6.3)
***n* = 429,775**	**3,041.2 (± 96.1)**

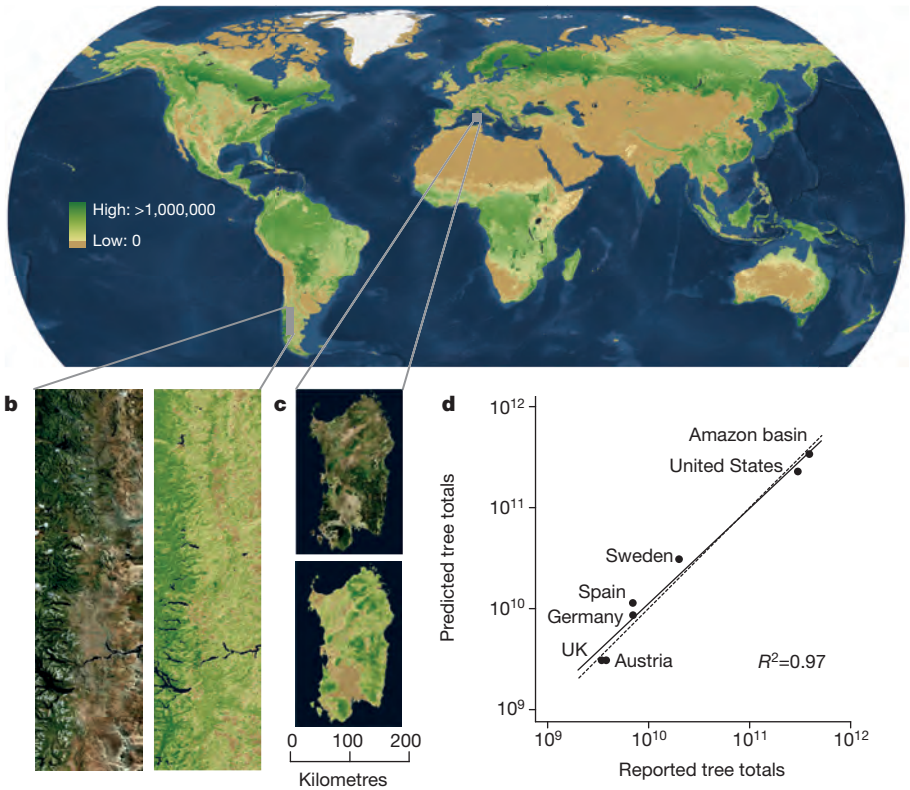

Figure 4 | The global map of tree density at the 1-km^2 pixel (30 arc-seconds) scale. **a**, The scale refers to the number of trees in each pixel. **b**, **c**, We highlight the map predictions for two areas (South American Andes (**b**) and Sardinia (**c**)) and include the corresponding images for visual comparison. All maps and images were generated using ESRI basemap imagery. **d**, A scatterplot as validation for our broad-scale estimates of total tree number. This shows the relationship between our predicted tree estimates and reported totals for regions with previous broad-scale tree inventories (see Methods for details). The straight line and the dotted line are the predicted best fit line and the 1:1 line, respectively.

by approximately 45.8% since the onset of human civilization (post-Pleistocene).

Discussion

The global map of tree density can facilitate ongoing efforts to understand biogeochemical Earth system dynamics[3,6,7,9] by incorporating ecosystem features that relate to elemental cycling rates[9,10]. For example, tree abundance can help to explain some of the variation in carbon storage and productivity within ecosystem types[7,9], but the strength of these effects remain untested across biomes[8]. We assessed the relationship between tree density and plant carbon storage at a global scale by regressing our plot-level tree counts against modelled estimates of plant biomass carbon in those sites[24]. This revealed a positive effect of tree density on plant carbon storage ($P < 0.001$). However, the strength of the relationship is weak ($r^2 = 0.14$), reflecting the vast array of local ecological forces that can obscure such global trends. For example, the effect of tree density is likely to interact strongly with tree size. Larger trees contain the greatest proportion of carbon in woodlands[25], but the highest tree densities within a given ecosystem type are often associated with young or recovering forests characterized by many small trees[13,20]. A thorough understanding of total vegetative carbon storage requires information about both the size and the number of individual trees.

A dense forest environment is a fundamentally different ecosystem from a sparse one and this influences a vast array of biotic and abiotic processes[10–12]. Current remote sensing tools capture some, but not all of this information. The tree density layer that we provide can therefore augment the currently available layers by providing unique insights into ecological dynamics that are not represented by estimates of forest cover or biomass[3,5,6]. It can inform biodiversity estimates and species distribution models by capturing perceivable environmental characteristics that determine habitat suitability for a wide variety of plants and animals[11–13]. Baseline estimates of tree populations are also critical for projecting population- and community-level tree demographics under current and future climate change scenarios[26], and for guiding local, national, and international reforestation/afforestation efforts[14–17]. Finally, by allowing us to comprehend the global forest extent in terms of tree numbers, this map contributes to our fundamental understanding of the Earth's terrestrial system.

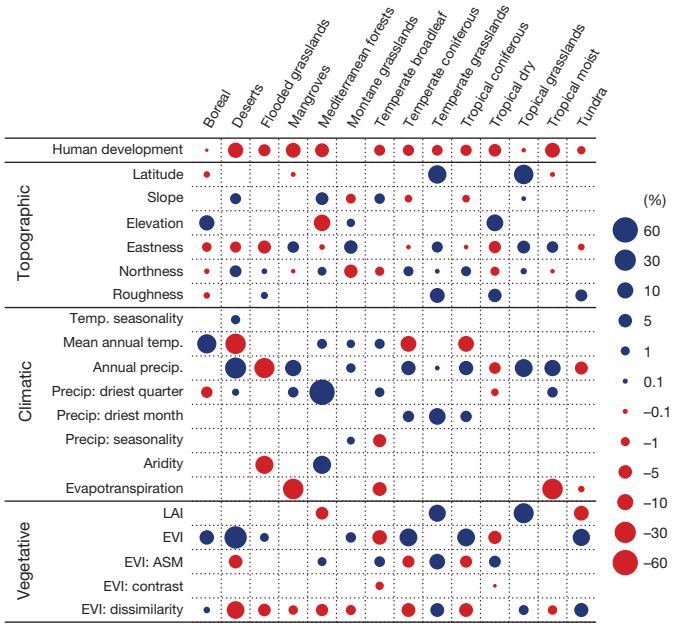

Figure 5 | Standardized coefficients for the variables included in final biome-level regression models. Coefficients represent relative per cent change in tree density for one standard deviation increase in the variable. Red and blue circles indicate negative and positive effects on tree density, respectively. Circle size indicates the magnitude of effects. All layers are available at the global scale. Human development = per cent developed and managed land; LAI = leaf area index; EVI = enhanced vegetation index; EVI: ASM = angular second moment of EVI; EVI: contrast = contrast of EVI; and EVI: dissimilarity = dissimilarity of EVI (see Extended Data Table 1).

Online Content Methods, along with any additional Extended Data display items and Source Data, are available in the online version of the paper; references unique to these sections appear only in the online paper.

Received 6 May; accepted 23 July 2015.

Published online 2 September; corrected online 9 September 2015 (see full-text HTML version for details).

1. Pan, Y. *et al.* A large and persistent carbon sink in the world's forests. *Science* **333,** 988–993 (2011).
2. Crowther, T. W. *et al.* Predicting the responsiveness of soil biodiversity to deforestation: a cross-biome study. *Glob. Change Biol.* **20,** 2983–2994 (2014).
3. Hansen, M. C. *et al.* High-resolution global maps of 21st-century forest cover change. *Science* **342,** 850–853 (2013).
4. Bonan, G. B. Forests and climate change: forcings, feedbacks, and the climate benefits of forests. *Science* **320,** 1444–1449 (2008).
5. Pfeifer, M., Disney, M., Quaife, T. & Marchant, R. Terrestrial ecosystems from space: a review of earth observation products for macroecology applications. *Glob. Ecol. Biogeogr.* **21,** 603–624 (2012).
6. Tuanmu, M.-N. & Jetz, W. A global 1-km consensus land-cover product for biodiversity and ecosystem modelling. *Glob. Ecol. Biogeogr.* **23,** 1031–1045 (2014).
7. Walker, A. P. *et al.* Predicting long-term carbon sequestration in response to CO_2 enrichment: how and why do current ecosystem models differ? *Glob. Biogeochem. Cycles* **29,** 476–495 (2015).
8. Asner, G. P. *et al.* A universal airborne LiDAR approach for tropical forest carbon mapping. *Oecologia* **168,** 1147–1160 (2012).
9. Fauset, S. *et al.* Hyperdominance in Amazonian forest carbon cycling. *Nature Commun.* **6,** 6857 (2015).
10. Slik, J. W. F. *et al.* Environmental correlates of tree biomass, basal area, wood specific gravity and stem density gradients in Borneo's tropical forests. *Glob. Ecol. Biogeogr.* **19,** 50–60 (2010).
11. Leathwick, L. R. & Austin, M. P. Competitive interactions between tree species in New Zealand old-growth indigenous forests. *Ecology* **82,** 2560–2573 (2001).
12. Oliver, C. D. & Larson, B. C. *Forest Stand Dynamics* (John Wiley & Sons, 1996).
13. Riginos, C. & Grace, J. B. Savanna tree density, herbivores, and the herbaceous community: bottom-up vs. top-down effects. *Ecology* **89,** 2228–2238 (2008).
14. O'Neil-Dunne, J., MacFaden, S. & Royar, A. A versatile, production-oriented approach to high-resolution tree-canopy mapping in urban and suburban landscapes using GEOBIA and data fusion. *Remote Sens.* **6,** 12837–12865 (2014).
15. Guldin, R. W. Forest science and forest policy in the Americas: building bridges to a sustainable future. *For. Policy Econ.* **5,** 329–337 (2003).
16. Cao, S. *et al.* Greening China naturally. *Ambio* **40,** 828–831 (2011).
17. Oldfield, E. E. *et al.* Growing the urban forest: tree performance in response to biotic and abiotic land management. *Restoration Ecol.* (http://dx.doi.org/10.1111/rec.12230) (2015).
18. Nadkarni, N. *Between Earth and Sky: Our Intimate Connections to Trees* (Univ. of California Press, 2008).
19. ter Steege, H. *et al.* Hyperdominance in the Amazonian tree flora. *Science* **342,** 1243092 (2013).
20. Bonan, G. B. & Shugart, H. H. Environmental factors and ecological processes in boreal forests. *Annu. Rev. Ecol. Syst.* **20,** 1–28 (1989).
21. Meyfroidt, P. & Lambin, E. F. Global forest transition: prospects for an end to deforestation. *Annu. Rev. Environ. Resour.* **36,** 343–371 (2011).
22. Rudel, T. K. The national determinants of deforestation in sub-Saharan Africa. *Phil. Trans. R. Soc. Lond. B* **368,** 20120405 (2013).
23. Hengeveld, G. M. *et al.* A forest management map of European forests. *Ecol. Soc.* **17,** 53 (2012).
24. Kindermann, G. E., McCallum, I., Fritz, S. & Obersteiner, M. A global forest growing stock, biomass and carbon map based on FAO statistics. *Silva Fennica* **42,** 387–396 (2008).
25. Stephenson, N. L. *et al.* Rate of tree carbon accumulation increases continuously with tree size. *Nature* **507,** 90–93 (2014).
26. Zhu, K., Woodall, C. W., Ghosh, S., Gelfand, A. E. & Clark, J. S. Dual impacts of climate change: forest migration and turnover through life history. *Glob. Change Biol.* **20,** 251–264 (2014).

Supplementary Information is available in the online version of the paper.

Acknowledgements We thank P. Peterkins for her support throughout the study. We also thank Plant for the Planet for initial discussions and for collaboration during the study. The main project was funded by grants to T.W.C. from the Yale Climate and Energy Institute and the British Ecological Society. We acknowledge various sources for tree density measurements and estimates: the Canadian National Forest Inventory (https://nfi.nfis.org/index.php), the US Department of Agriculture Forest Service for their National Forest Inventory and Analysis (http://fia.fs.fed.us/), the Taiwan Forestry Bureau (which provided the National Vegetation Database of Taiwan), the DFG (German Research Foundation), BMBF (Federal Ministry of Education and Science of Germany), the Floristic and Forest Inventory of Santa Catarina (IFFSC), the National Vegetation Database of South Africa, and the Chilean research grants FONDECYT no. 1151495. For Europe NFI plot data were brought together with input from J. Rondeux and M. Waterinckx, Belgium, T. Bélouard, France, H. Polley, Germany, W. Daamen and H. Schoonderwoerd, Netherlands, S. Tomter, Norway, J. Villanueva and A. Trasobares, Spain, G. Kempe, Sweden. New Zealand Natural Forest plot data were collected by the LUCAS programme for the Ministry for the Environment (New Zealand) and sourced from the National Vegetation Survey Databank (New Zealand) (http://nvs.landcareresearch.co.nz). We also acknowledge the BCI forest dynamics research project, which was funded by National Science Foundation grants to S. P. Hubbell, support from the Center for Tropical Forest Science, the Smithsonian Tropical Research Institute, the John D. and Catherine T. MacArthur Foundation, the Mellon Foundation, the Small World Institute Fund, numerous private individuals, the Ucross High Plains Stewardship Initiative, and the hard work of hundreds of people from 51 countries over the past two decades. The plot project is part of the Center for Tropical Forest Science, a global network of large-scale demographic tree plots.

Author Contributions The study was conceived by T.W.C and G.H. and designed by T.W.C., K.R.C. and M.A.B. Statistical analyses were conducted by H.B.G., S.M.T., J.R.S., C.B., D.S.M. and T.W.C and mapping was conducted by H.B.G. and C.B. The manuscript was written by T.W.C. with input from M.A.B., P.C., D.S.M., H.B.G. and C.B., with comments provided by all other authors. Tree density measurements or geospatial data from all over the world were contributed by K.R.C., S.M.T., M.C.D., G.A., M.N.T., W.J., C.Sa., C.St., D.P., T.T., S.G., G.B., S.J.W., S.K.W., M.O.H., G.M.H., G.J.N., E.T., P.B., C.F.L., L.W.P., M.F., A.H., J.H., P.C., A.C.V., P.M.U., S.L.P., C.W.R. and M.S.A.

Author Information Reprints and permissions information is available at www.nature.com/reprints. The authors declare no competing financial interests. Readers are welcome to comment on the online version of the paper. Correspondence and requests for materials should be addressed to T.W.C. (thomas.crowther11@gmail.com).

METHODS

Data collection and standardisation. Plot-level data were collected from international forestry databases, including the Global Index of Vegetation-Plot Database (GIVD http://www.givd.info), the Smithsonian Tropical Research Institute (http://www.stri.si.edu), ICP-Level-I plot data which covers most of Europe (http://www.icp-forests.org), and National Forest Inventory (NFI) analyses from 21 countries, including the USA (http://fia.fs.fed.us/) and Canada (https://nfi.nfis.org/index.php). This information was supplemented with data from peer-reviewed studies reporting large international inventories published in the last 10 years (collected using ISI Web of Knowledge, Google Scholar and secondary references)[19,27,28].

We only included density estimates where individual trees met the criterion of ≥10 cm diameter at breast height (DBH). Although NFI databases can vary slightly in their definition of a mature tree (for example, the US Forest Service Forest Inventory and Analysis (FIA)[29] defines a tree as a plant with woody stems larger than 12.7 DBH) the vast majority of sources use 10 cm as the DBH cut-off. Indeed, this was the only size class provided by all broad-scale inventories (including the FIA), so density estimates at other DBH values were excluded. This provided a total of 429,775 measurements of forest tree density (each generated at the hectare scale) that were then linked to spatially explicit remote-sensing data and GIS variables to explore the patterns in forest tree density at a global scale. The scale of our plot data (in terms of number and distribution of plots) ensured that any plot location uncertainty or minor changes in global forest area are unlikely to alter mean values or modelled estimates.

Acquisition and preprocessing of spatial data. For predictive model development, we selected 20 geospatial covariates from a larger pool of potential covariates based on uniqueness, spatial resolution and ecological relevance (Extended Data Table 1). Covariates were derived through satellite-based remote sensing and ground-based weather stations, and can be loosely grouped into one of four categories: topographic, climatic, vegetative or anthropogenic. Topographic covariates included elevation, slope, aspect (as northness and eastness), latitude (as absolute value of latitude) and a terrain roughness index (TRI). Climatic covariates included annual mean temperature, temperature annual range, annual precipitation, precipitation of driest month, precipitation seasonality (coefficient of variation), precipitation of driest quarter, potential evapotranspiration per hectare per year, and indexed annual aridity. Vegetative covariates included, enhanced vegetation index (EVI), leaf area index (LAI), dissimilarity, contrast, and angular second moment. We also included a single anthropogenic covariate: proportion of urban and/or developed land cover (see Extended Data Table 1).

Several covariates bear special mention. Moving-window analyses were applied to an EVI derived from a multi-year composite of moderate resolution imaging spectroradiometer (MODIS) imagery. From the result, we extracted three second-order textural covariates that reflect the heterogeneity of vegetation, intended to capture difference in vegetative structure. These include angular second moment (the orderliness of EVI among adjacent pixels), contrast (the exponentially weighted difference in EVI between adjacent pixels: see http://earthenv.org for details), and dissimilarity (difference in EVI between adjacent pixels). Terrain roughness index (the mean of absolute differences between a cell and its adjacent neighbours) was derived from aggregated Global Multi-Resolution Terrain Elevation Data of 2010. Terrain roughness index was computed using the eight neighbouring pixels, while the others were computed using the four neighbouring pixels located at 0°, 45°, 90°, 135° (see http://earthenv.org and ref. 36 for details).

We preprocessed all spatial covariates using ArcMap 10.1 (ESRI, Redlands, CA, 2012) and RStudio 0.97.551 (RStudio, 2012). All covariates were reprojected to the interrupted Goode Homolosine equal-area coordinate system (which maximises spatial precision by amalgamating numerous region-specific equal-area projections) to optimize the areal accuracy of our final figures[30]. These were then resampled to match the coarsest resolution used during analysis (nominal 1 km^2 pixels), and spatially coregistered using nearest neighbour resampling where necessary.

To account for broad-scale differences in vegetation types, we developed spatial models at the biome scale. Individual predictive models were generated within each of 14 broad ecosystem types (delineated by the Nature Conservancy http://www.nature.org) to improve the accuracy of estimates.

Statistical modelling. We used generalized linear models to generate predictive maps of tree numbers within forested ecosystems for each biome. This approach also enabled us to explore the mechanisms potentially governing patterns in forest tree density within regions (Fig. 5). Due to the inherently interactive nature of climate, soil and human impact factors across the globe, we predicted that there would be pronounced non-independence within the full suite of biophysical variables extracted from the compiled GIS layers. To account for this colinearity, we performed ascendant hierarchical clustering using the *hclustvar* function in R's *ClustOfVar* package[31] in each biome-level model. This analysis splits the variables into different clusters (similar to principal components) in which all variables correlate with one another. A single best 'indicator' variable is then selected from each cluster, based on squared loading values representing the correlation with the central synthetic variable of each cluster (that is, the first principal component of a PCAmix analysis). This set of 'best' indicator variables for each biome was then included in all subsequent models used to estimate controls on forest tree density.

Using the resulting set of variables, we constructed generalized linear models with a negative binomial error structure (to account for count data that could not extend below zero) for each biome (Extended Data Figs 1, 2 and 3) and performed a multi-model dredging using the dredge function in R's MuMIn package[32]. This function constructs all possible candidate sub-models nested within the global model, identifies the most plausible subset of models for each data set, and then ranks them according to corrected Akaike Information Criterion (AICc) values and AIC likelihood weights (AICcw). We derived covariates, coefficients, and variance-covariance matrices for biome-level models through weighted model averaging the dredged model results with cumulative AIC weights at least equal to 0.95 (ref. 33). Given the inherent sampling bias present in our plot data (tree density estimates were only collected in forested ecosystems and non-forested regions are under-represented), our modelling approach was used to generate predictive estimates of forest tree density, and these estimates were subsequently scaled based on the total area of forested land in each pixel (see spatial modelling for details).

Model validation and testing. We assessed the model fit by investigating the bias and precision present when predicting mean tree density across an aggregate number of plots. This approach allowed us to test how many plots are required to ensure that the predicted mean (or total) forest density has reasonable bias and precision. 20% of the plots within each biome were randomly omitted before model fitting to serve as an independent data set for model testing. Initial model validation was conducted using the biome-specific regression models (obtained from the remaining 80% of the data) to predict the tree density for each omitted plot. The mean predicted tree density of the omitted data was then regressed against the mean observed tree density of the omitted data for each biome (Fig. 2). In addition, a bootstrapping algorithm was used to quantify the standard deviation of the mean prediction as a function of sample size following ref. 34. For each biome, we generated empirical bootstrap estimates of the standard deviation of the predicted mean using random samples drawn from the withheld validation plots. Specifically, for each biome a bootstrap sample of size n was selected, with replacement, from the omitted data in that biome. The fitted regression model for that biome (based on the 80% retained data) was used to predict the tree density of each point, and the mean of the n samples was calculated. This process was repeated 10,000 times for each sample size ($n = 10, 20, \ldots, 500$) and in each case the empirical standard deviation of the 10,000 sample mean was calculated and plotted (Fig. 2). Where the number of plot records in a biome fell below the sample size threshold identified through bootstrapping, we used models from the most similar biome available (in terms of phylogenetic relatedness of the dominant tree species and mean tree density from the few plot values collected). This was the case for the two smallest biomes: 'mangroves' (0.23% of land surface) and 'tropical coniferous' (0.46% of land surface) forests, which used models from 'tropical moist' and 'temperate coniferous', respectively.

Spatial modelling. Following model averaging and bootstrapping, we applied the final negative binomial regression equations used in bootstrapping to pixel-level spatial data at the biome level. Regressions were run in a map algebra framework wherein equation intercepts and coefficients were applied independently to each pixel of our coregistered global covariates to produce a single map of forest tree density on a per-hectare scale. We then scaled our per-hectare forest density estimates to the 1-km^2 scale based on the total area of forested land within each pixel, as estimated by the global 1-km consensus land cover data set for 2014 (ref. 6). This process was then validated using an older (2013) data set that used fine-scale (30 m) forest cover information[3], which revealed equivalent total tree counts. By multiplying our predicted forest density by the area of forest, we ensured that we did not overestimate tree densities in non-forested sites. From the resulting maps, summary statistics (mean tree density, total tree number) were derived for each polygonal area of interest. The variances of the global and biome-specific totals were calculated using a Taylor series approximation to account for the log-link negative binomial regression function and correlation among the regression-based predicted values[35].

By generating models at the biome-level, we were able to account for broad-scale differences in vegetation types between biomes, while maintaining high precision of our mean (and total) estimates at the global scale (due to the high

number of plot measurements within biomes). However, biome-level models are limited in their accuracy when predicting tree density at fine-scales, which might ultimately have the potential to alter final numbers. We therefore constructed models within each of 813 global ecoregions (delineated by the Nature Conservancy http://www.nature.org) as a validation for the first biome-level approach. We generated models and estimated tree numbers using exactly the same approach as for the biome-level models. Total, and biome-level, tree estimates did not differ significantly ($P < 0.05$) from those generated using the biome-level models (Extended Data Fig. 4).

27. Lewis, S. L. *et al.* Above-ground biomass and structure of 260 African tropical forests. *Phil. Trans. R. Soc. Lond. B* **368,** 20120295 (2013).
28. Brus, D. J. *et al.* Statistical mapping of tree species over Europe. *Eur. J. For. Res.* **131,** 145–157 (2011).
29. USDA Forest Service. Forest Inventory and Analysis National Program http://fia.fs.fed.us/ (2010).
30. Steinwand, R. S., Hutchinson, J. A. & Snyder, J. P. Map projections for global and continental data sets and an analysis of pixel distortion caused by reprojection. *Photogramm. Eng. Remote Sensing* **61,** 1487–1499 (1995).
31. Chavent, M., Kuentz, V., Liquet, B. & Saracco, J. ClustOfVar: an R package for the clustering of variables. *J. Stat. Softw.* **50,** 1–16, http://www.jstatsoft.org/v50/i13/ (2012).
32. Bartoń, K. MuMIn: Model selection and model averaging based on information criteria (AICc and alike). (https://cran.r-project.org/web/packages/MuMIn/index.html) (2015).
33. MacKenzie, D. I. *et al. Occupancy Estimation and Modeling* (Academic Press, 2005).
34. MacLean, M. G. *et al.* Requirements for labelling forest polygons in an object-based image analysis classification. *Int. J. Remote Sens.* **34,** 2531–2547 (2013).
35. Ståhl, G. *et al.* Model-based inference for biomass estimation in a LiDAR sample survey in Hedmark County, Norway. *Can. J. For. Res.* **41,** 96–107 (2011).
36. Tuanmu, M.-N. & Jetz, W. A global, remote sensing-based characterization of terrestrial habitat heterogeneity for biodiversity and ecosystem modelling. *Glob. Ecol. Biogeogr.* http://dx.doi.org/10.1111/geb.12365 (2015).

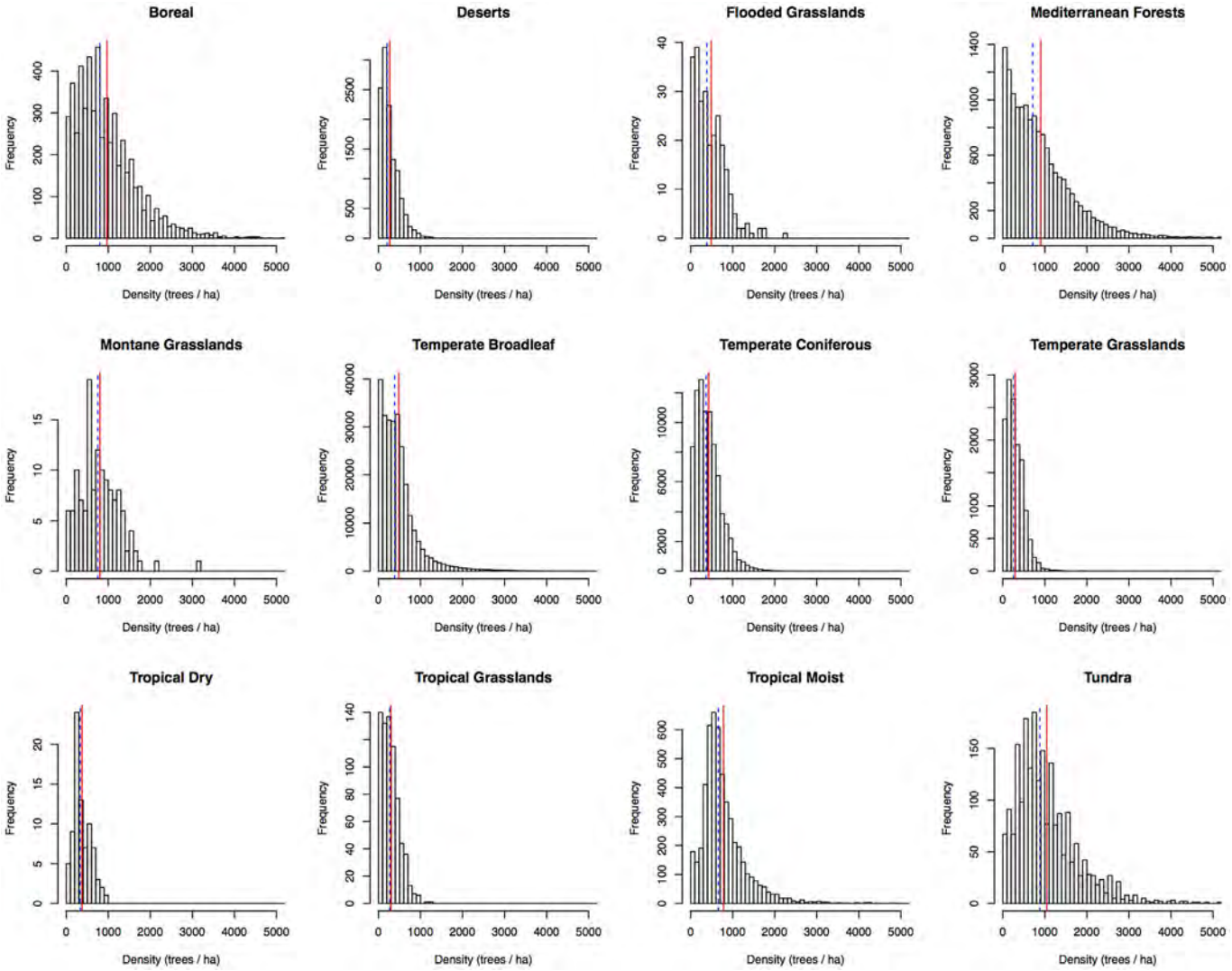

Extended Data Figure 1 | Histogram of the collected measurements of forest tree density in each biome around the world ($n = 429{,}775$). The red line and the blue dotted lines indicate the mean and median for the collected data, respectively. Data in each biome fitted a negative binomial error structure.

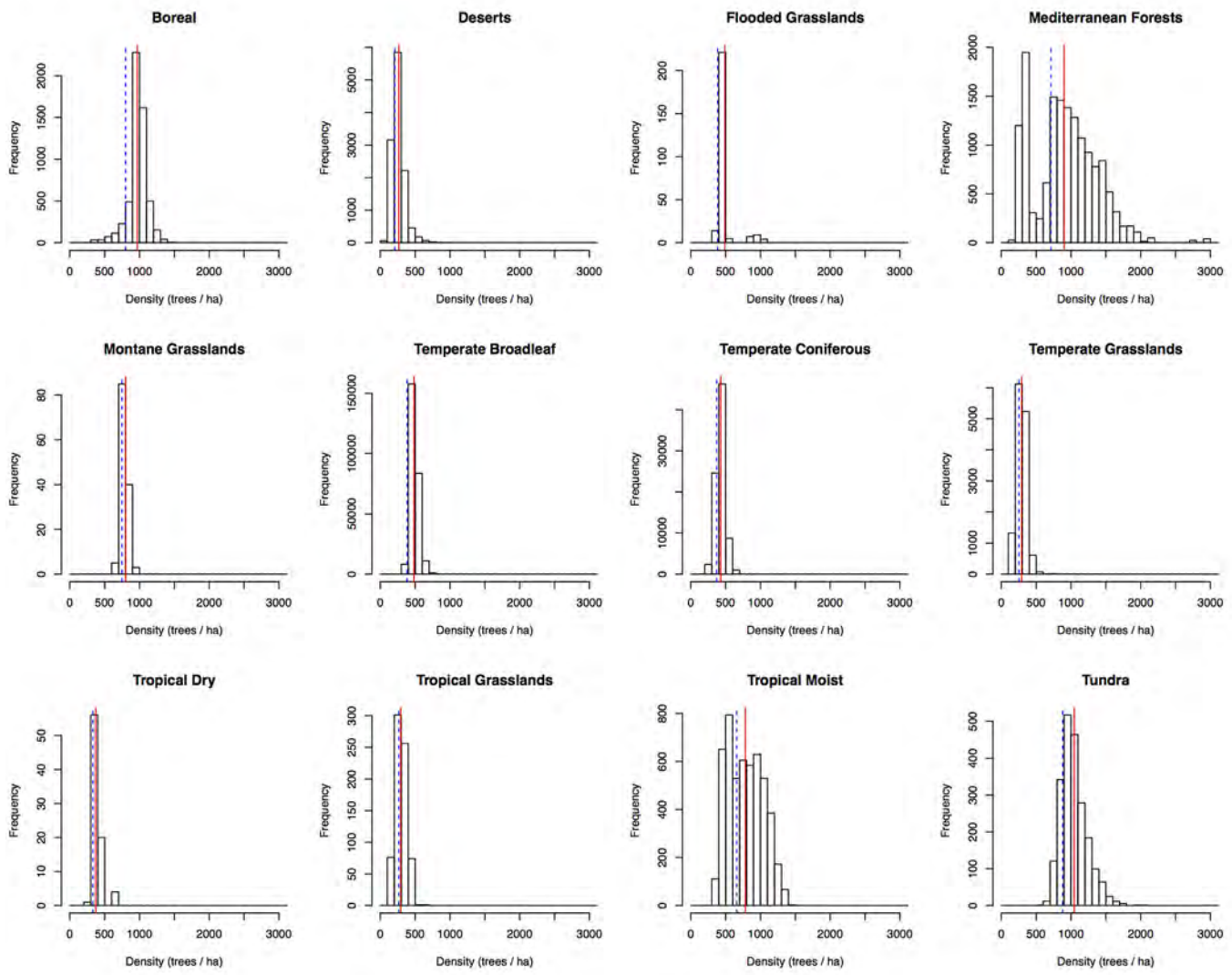

Extended Data Figure 2 | Histogram of the predicted forest tree density values for the locations that density measurements were collected in each biome around the world ($n = 429{,}775$). The red line and the blue dotted lines indicate the mean and median for the collected data, respectively. As our models were based on mean values, the majority of points fall on or close to the mean values in each biome.

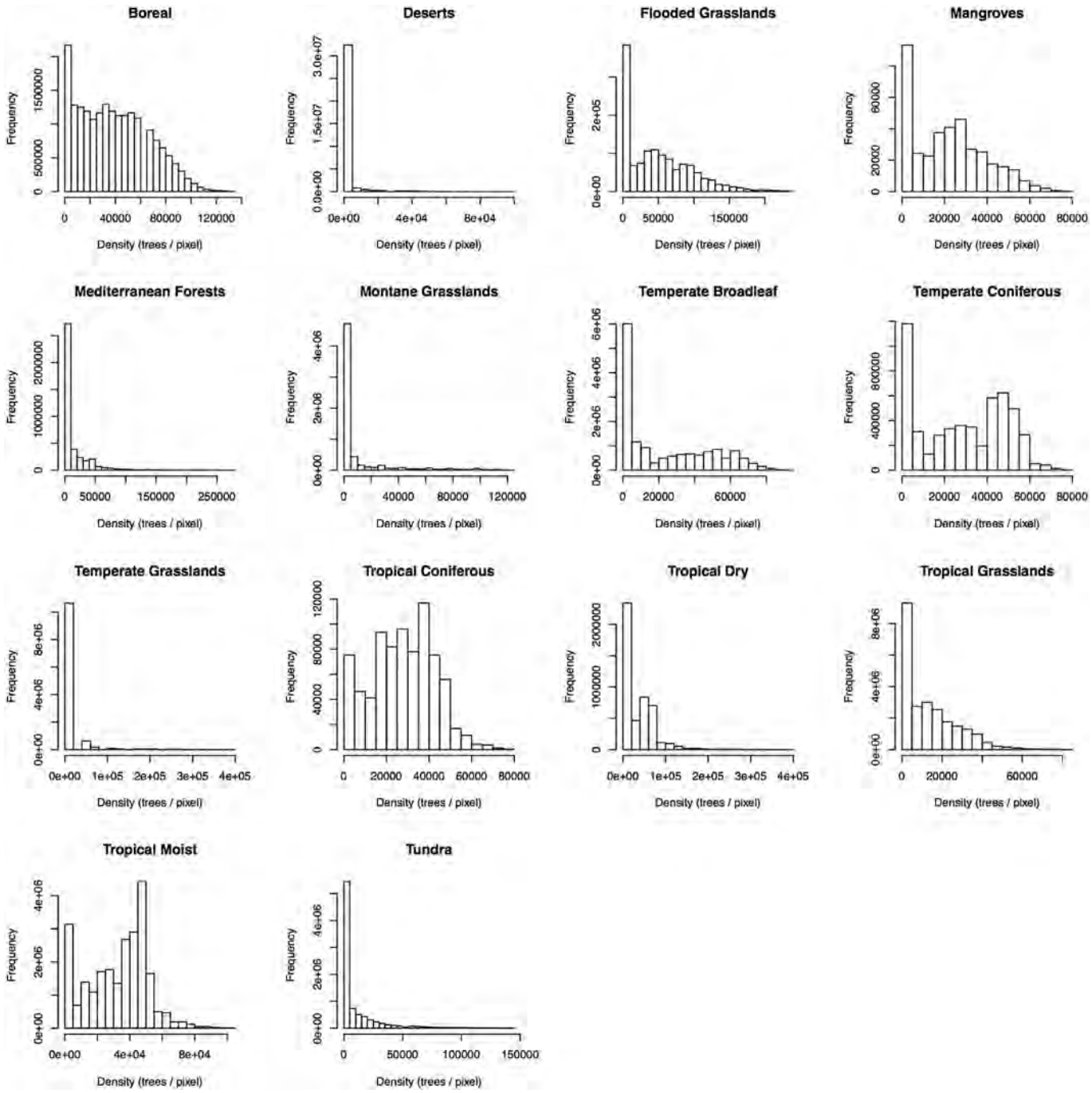

Extended Data Figure 3 | Histogram of the total predicted forest tree density values for each pixel within each biome around the world ($n = 429{,}775$). This illustrates the spread of pixels throughout each biome, and highlights that our map accounts for the sampling bias in tree density plots (for example, although we had no zero values in our desert plots, the vast majority of desert pixels contain no trees).

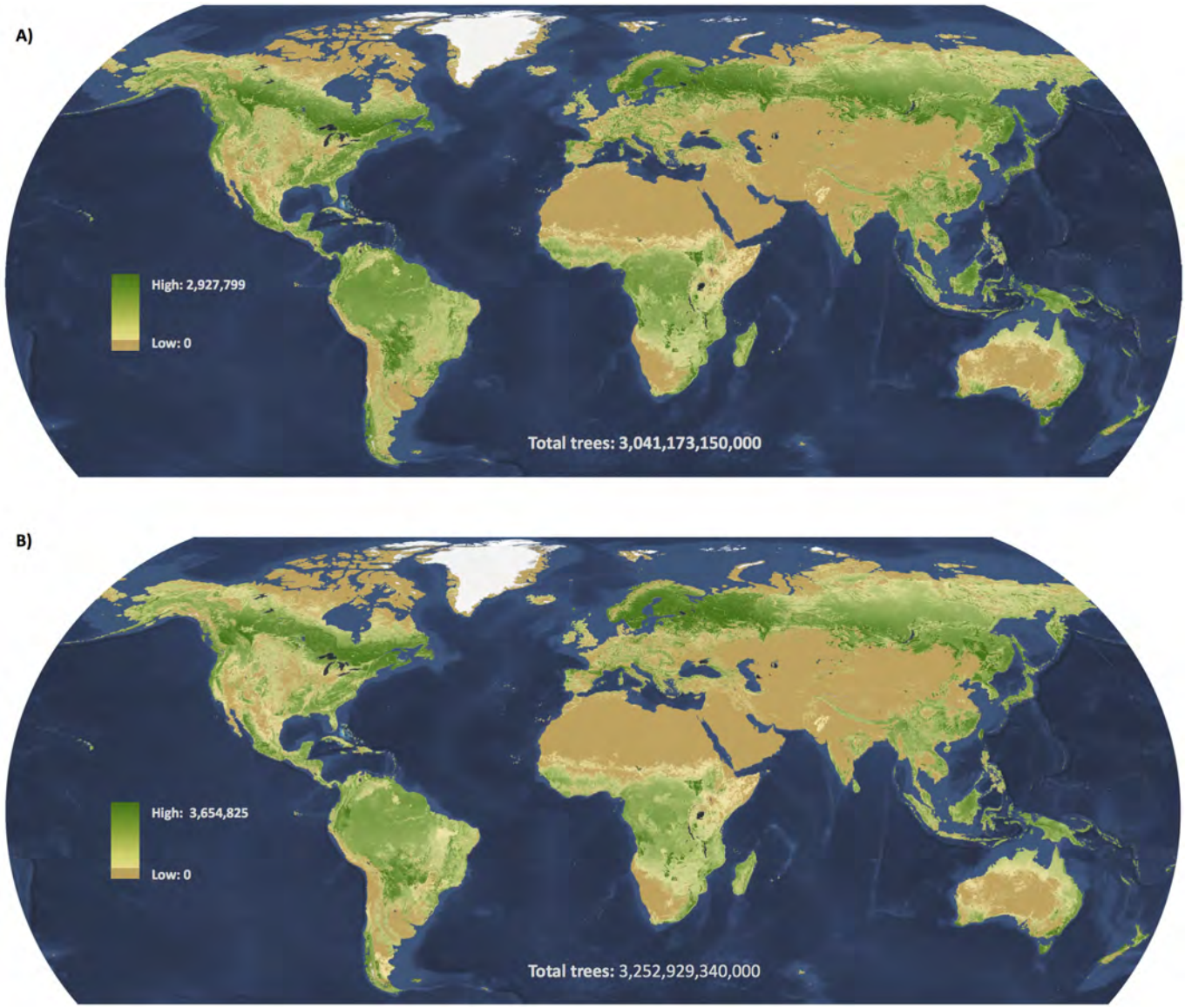

Extended Data Figure 4 | Comparison between approaches to generate the global tree density map. The initial map was generated using 14 biome-level models (biomes delineated by The Nature Conservancy http://www.nature.org) to account for broad-scale variations in terrestrial vegetation types. With several thousand plot-level density measurements in most biomes, this approach provided highly accurate estimates at the global scale. However, to improve precision at the local scale, we also generated a map using ecoregion-scale models. Separate models were generated within each of 813 global ecoregions (also delineated by The Nature Conservancy to reflect smaller-scale vegetation types) using exactly the same statistical approach (see Methods). The same 429,775 data points were used to construct each map. Biome-level and ecoregion-level maps provide total tree estimates of 3.041 and 3.253 trillion trees, respectively.

Extended Data Table 1 | Estimates of the total tree number for each of the biomes that contain forested land, as delineated by The Nature Conservancy (http://www.nature.org)

Biome	% Total Land Area	n	Total Trees (Billions)	± 2 SD (Billions)	% Total Trees
Boreal Forests	11.49%	8688	749.34	50.07	24.28%
Deserts	21.01%	14637	52.95	2.92	1.75%
Flooded Grasslands	0.79%	271	64.58	14.19	2.13%
Mangroves	0.23%	21	8.18	0.26	0.27%
Mediterranean Forests	2.43%	16727	53.42	1.20	1.76%
Montane Grasslands	3.88%	138	60.3	24.04	1.99%
Temperate Broadleaf	9.32%	278395	362.6	2.90	11.98%
Temperate Conifer	3.18%	85144	150.57	1.34	4.97%
Temperate Grasslands	7.18%	17051	148.29	4.93	4.90%
Tropical Coniferous	0.48%	0	22.21	0.40	0.73%
Tropical Dry	2.85%	115	156.37	63.42	5.17%
Tropical Grasslands	14.66%	999	318.01	35.52	10.51%
Tropical Moist	14.81%	5321	799.45	23.98	26.41%
Tundra	5.25%	2268	94.89	6.31	3.14%
Total		**429775**	**3041.17**	**96.07**	